

Quantum speedup from nonclassical polarization

Tim Aßbrock,* Jan Sperling, and Laura Ares

*Theoretical Quantum Science, Institute for Photonic Quantum Systems (PhoQS),
Paderborn University, Warburger Straße 100, 33098 Paderborn, Germany*

(Dated: March 25, 2026)

We develop a framework for identifying nonclassical speedups in systems with polarization, likewise spin degrees of freedom. By confining the dynamics to the manifold of angular momentum coherent states, which act as the classical reference in this case, we compute the speed limit that bounds the rate of change of the state achievable without generating quantum coherence. A comparison with the unrestricted quantum speed limit enables the quantitative identification of speedups arising from polarization nonclassicality. We apply this framework to the cross-Kerr interaction, demonstrating a persistent speedup scaling as $\mathcal{O}(\sqrt{N})$ with the photon number N . The results establish polarization nonclassicality as a genuine dynamical resource, linking quantum coherence to quantum-enhanced evolution speeds in nonlinear photonic systems.

I. INTRODUCTION

Quantum physics is the framework describing physical phenomena at microscopic scales, where superposition, interference, and entanglement are the governing elements determining the structure and evolution of matter and radiation [1–4]. Beyond the fundamental insight into nature, quantum mechanics constitutes the foundation for a wide range of research areas, from quantum optics, over condensed-matter physics, to quantum thermodynamics [5–8]. In each of these different fields, controlled access to quantum states and their dynamics has not only enabled precision tests of physical laws but also furthered the development of emerging quantum technologies [9–12]. Within this larger landscape, quantum information science has established itself as a central discipline, systematically exploring how quantum resources enable computation, secure communication, and metrology [1, 9, 13, 14], and providing an operational framework in which the conversion from one quantum resource to another plays a central role.

A key question across the aforementioned domains concerns the impact of quantum resources on the system’s dynamical behavior. Quantum speed limits (QSLs) formalize this question by bounding the maximal rate at which a system can change between distinct states for a given generator of the evolution, e.g., the Hamiltonian [10, 15–17]. These bounds play a dual role: They cast light on structural dynamical constraints in quantum theory and set performance limits for quantum information processing, including, for example, gate execution times, state-transfer protocols, and metrological sensitivity [17–19]. The landscape of QSLs stretches across several major directions. First, open-system and perturbed scenarios use QSLs to quantify deviations from reference trajectories and directly relate to quantum Fisher information and environmental time scales [20, 21]. Second, thermodynamic and stochastic formulations now bring

QSLs and thermodynamic uncertainty relations in a unifying picture [8]. Third, bounds for observables constrain the rate of change of expectation values, being important for entanglement generation, modular Hamiltonians, and quantum batteries [22, 23]. Non-Hermitian and measurement-induced dynamics introduce gain and loss channels and means for continuous monitoring into the QSLs [24], and anomalous transport and memory effects drive fractional-time generalizations for open systems [25]. At the many-body level, operator-flow and correlation-spreading QSLs complement Lieb-Robinson-type bounds by characterizing limits to scrambling and information propagation [26, 27]. A recurring theme across these developments is that genuinely quantum resources can accelerate thermodynamic processes, control operations, and information flow [28].

The promising field of photonic quantum technologies provides a particularly suitable context to investigate the quantum aspect of the dynamics because of low-loss transmission, resilience against decoherence, mature state-preparation techniques, and compatibility with existing optical infrastructure [5, 6, 11]. Polarization encoding, in particular, allows high-fidelity manipulation and interferometric stability [29, 30], naturally interfacing with multi-photon interference and entanglement generation [12, 31]. Moreover, recent theoretical and experimental work has further established a strict equivalence between polarization nonclassicality and multi-photon entanglement, thereby unifying two key signatures of quantumness within a single operational framework [32]. Thus, polarization photonic systems offer a platform where dynamical advantages induced by nonclassical resources can be quantitatively assessed via experimentally accessible observables. Yet, a theoretical analysis and methodology applicable to experiments in nonlinear polarization optics is missing to date.

In this work, we investigate how quantum resources manifest as dynamical advantages by comparing the temporal behaviour of polarization (likewise, spin) systems to the classical scenario in which nonclassical resources are not accessible. To this end, we derive equations of motion that confine the dynamics to the manifold of classical po-

* tim.assbrock@uni-paderborn.de

larization states, the so-called angular momentum coherent states (AMCSs), preventing the buildup of quantum coherence at all times [33]. AMCSs are a suitable classical reference since, being SU(2)-coherent states, minimize angular-momentum uncertainties and exhibit shot-noise-limited Stokes fluctuations, and directly relate to the coherent states of the harmonic oscillator, [34–36]. Furthermore, we compute the speed limits for the restricted dynamics, allowing for a direct comparison with the actual QSLs of the process and thereby assessing the advantages of nonclassical processes.

As an application, we apply our method to investigate the cross-Kerr effect, which arises from the third-order nonlinear susceptibility of the medium that leads to an intensity-dependent refractive index [37]. Cross-Kerr nonlinearities play a central role in quantum optics and quantum information science [38–40], enabling quantum nondemolition measurements [41], the realization of photonic controlled-phase gates [42, 43], and facilitating the generation of nonclassical states [40]. More broadly, cross-Kerr interactions represent a fundamental mechanism for implementing all-optical quantum logic operations [44]. See Refs. [45–48] for experimental applications. Our findings unambiguously link the quantum coherence generated by this nonlinear interaction to the speedup of the dynamics.

II. PRELIMINARIES

To establish a clear foundation for the forthcoming derivation, we briefly review some required concepts in this section. We begin by revisiting the notions of quantum coherence and AMCSs. Then, we summarize the procedure that restricts the dynamics to classical states, and specify the definition of the specific QSL for dynamical polarization nonclassicality.

A. Quantum coherence

We here adopt the resource-theoretic notion of quantum coherence presented in [49]. Throughout, quantum coherence is defined relative to a fixed set of reference states $|\psi(\mathbf{q})\rangle$, acting as the classical reference, where the tuple \mathbf{q} serves as the parametrization for such states [33]. A quantum state is then said to exhibit quantum coherence if it cannot be written as a convex mixture of these basis states. Within this framework, quantum coherence serves as the marker of nonclassicality, which can, for example, translate into the quasiprobability distribution representing the state showing negative values [50–55]. For instance, this notion of quantum coherence encompasses quantum effects like entanglement by choosing product states as the basis states.

B. Angular momentum coherent states

Now, we elaborate on the set of classical reference states for polarization. AMCSs are built on the Schwinger representation [56], introducing two independent bosonic modes with the creation operators \hat{a}_\pm^\dagger representing two orthogonal polarizations. These operators satisfy the canonical commutation relations and yield the angular momentum operators

$$\hat{J}_\pm = \hat{a}_\pm^\dagger \hat{a}_\mp = \hat{J}_x \pm i\hat{J}_y \quad \text{and} \quad \hat{J}_z = \frac{1}{2}(\hat{n}_+ - \hat{n}_-), \quad (1)$$

with $\hat{n}_\pm = \hat{a}_\pm^\dagger \hat{a}_\pm$ [34, 56]. The above operators form the ladder operators and spin- z operator for an angular momentum algebra, represented by the corresponding Stokes operators in quantum optics. In two-mode Fock basis $\{|n_+, n_-\rangle : n_\pm \in \mathbb{N}\}$, the AMCS $|s_N\rangle$ for a N -photon state with n_+ photons in the “+” mode and $n_- = N - n_+$ photons in the “-” mode is given by [32]

$$|s_N\rangle = \sum_{n_+=0}^N \binom{N}{n_+}^{\frac{1}{2}} \alpha_+^{n_+} \alpha_-^{n_-} |n_+, n_-\rangle, \quad (2)$$

with $|\alpha_+|^2 + |\alpha_-|^2 = 1$. In contrast to Glauber coherent states, AMCSs for N photons are not eigenstates of the annihilation operators \hat{a}_\pm ; but one can show that said operators act as

$$\hat{a}_\pm |s_N\rangle = \sqrt{N} \alpha_\pm |s_{N-1}\rangle, \quad (3)$$

effectively mapping the N -photon AMCS onto the corresponding $(N - 1)$ -photon state.

C. Classical evolution

The definition of classical evolution considered here forbids the presence of quantum coherence for all times t [33], in contrast with the common interpretation encompassing processes that map classical states into classical states via a Kraus operator after a certain time T . Based on the notion for the continuum of times, one can derive restricted equations of motion for a general process by imposing on the evolution the constraint to remain classical, which yields

$$\langle \nabla_{\mathbf{q}} \psi(\mathbf{q}) | (i\hbar \partial_t |\psi(\mathbf{q})\rangle - \hat{H} |\psi(\mathbf{q})\rangle) = \mathbf{0}. \quad (4)$$

Note that the vector $|\nabla_{\mathbf{q}} \psi(\mathbf{q})\rangle = \nabla_{\mathbf{q}} |\psi(\mathbf{q})\rangle$ is the derivative of the classical reference state with respect to its parametrization \mathbf{q} , i.e., tangent vectors to the manifold of classical states $|\psi(\mathbf{q})\rangle$ at point \mathbf{q} . Thus, Eq. (4) describes the common Schrödinger evolution projected onto the classical states. A comparison with the dynamics described by the actual - i.e., non-projected - Schrödinger equation allows us to isolate the temporal effect of nonclassicality in the evolution of states.

D. Quantum speed limit

Finally, we recall the concept of QSL, which characterizes the maximal rate of change of a quantum system evolving between two distinct states. Note that various formulations exist, e.g., the early Mandelstamm-Tamm bound and the Margolus-Levitin bound [15–18]. In this work, we utilize the geometric approach to QSLs, where the instantaneous speed of evolution is identified with the trace-norm of the rate of change of the density operator, which quantifies the infinitesimal change in state distinguishability [17, 57, 58].

Explicitly, for a quantum state $|\Psi\rangle\langle\Psi|$, the rate of change is given by $\|\partial_t |\Psi\rangle\langle\Psi|\|_1$, where $\|\dots\|_1$ is the trace norm, equivalently defined as the sum of the modulus of the eigenvalues of a self-adjoint operator. The QSL is then the maximal rate of change of the system [17, 57],

$$\text{QSL} = \sup_{|\Psi\rangle} \|\partial_t |\Psi\rangle\langle\Psi|\|_1 = \sup_{|\Psi\rangle} \left\| \frac{1}{i\hbar} [\hat{H}, |\Psi\rangle\langle\Psi|] \right\|_1. \quad (5)$$

Note that, in closed systems, we can limit the study to pure states because of convexity. The rate of change can be directly linked to the dynamics' generator, the Hamiltonian \hat{H} , and thus to the energy of the system, through the von Neumann equation [18]. The QSL for the quantum dynamics without any constraint on the evolution results in

$$\text{QSL} = \frac{E_{\max} - E_{\min}}{\hbar}, \quad (6)$$

where E_{\max} and E_{\min} denote the supremum and infimum over $|\Psi\rangle$ of the energy values $E = \langle\Psi|\hat{H}|\Psi\rangle$, respectively; see, for example, Ref. [18] and references therein for detailed derivations.

III. RESTRICTED FRAMEWORK

In this section, we restrict the dynamics of a general Hamiltonian to classical states for polarization systems and compute the thereby restricted speed limit. This constitutes a general framework, allowing for the certification of polarization-nonclassical processes, which then can be applied to concrete processes; see next section.

A. Equations of motion

We derive the equations of motion constrained to AMCSs by introducing $|s_N\rangle$ in the Schrödinger-type equation of motion, Eq. (4). According to Eq. (2), we identify the classical parametrization as $\mathbf{q} = \boldsymbol{\alpha} = (\alpha_+, \alpha_-) \in \mathbb{C}^2$, being the only varying parameters in $|s_N\rangle$. Thus, the time derivative of the AMCS takes the form

$$\partial_t |s_N\rangle = \sqrt{N} \left(\dot{\alpha}_+ \hat{a}_+^\dagger + \dot{\alpha}_- \hat{a}_-^\dagger \right) |s_{N-1}\rangle, \quad (7)$$

where the dot notation, $\dot{\alpha}_\pm = \partial_t \alpha_\pm$, and the identity in Eq. (3) were used. Further, we can rewrite $\langle\nabla_{\boldsymbol{\alpha}} s_N | \hat{H} |s_N\rangle = \nabla_{\boldsymbol{\alpha}^*} \langle s_N | \hat{H} |s_N\rangle$ since neither \hat{H} nor $|s_N\rangle$ depend on α_\pm^* . Substituting the above expressions into Eq. (4), we obtain the following coupled equations of motion

$$\begin{pmatrix} \dot{\alpha}_+ \\ \dot{\alpha}_- \end{pmatrix} = -\frac{i}{\hbar N^2} \boldsymbol{\Lambda} \begin{pmatrix} \partial_{\alpha_+^*} \langle \hat{H} \rangle \\ \partial_{\alpha_-^*} \langle \hat{H} \rangle \end{pmatrix}, \quad (8)$$

for each component of $\boldsymbol{\alpha} = (\alpha_+, \alpha_-)$ and with $\langle \hat{H} \rangle = \langle s_N | \hat{H} |s_N\rangle$ and the $\boldsymbol{\alpha}$ -dependent matrix

$$\boldsymbol{\Lambda} = \begin{pmatrix} 1 + (N-1)|\alpha_-|^2 & -(N-1)\alpha_-^* \alpha_+ \\ -(N-1)\alpha_+^* \alpha_- & 1 + (N-1)|\alpha_+|^2 \end{pmatrix}. \quad (9)$$

These equations of motion formally resemble Hamilton's equations in classical mechanics, but with respect to a quantum-state-dependent symplectic structure that arises from the restriction to the manifold of AMCSs [59]. Moreover, Eqs. (8) and (9) can be equivalently reformulated in terms of the normalized, classical Stokes vector

$$\vec{r} = \frac{2}{N} \langle \vec{J} \rangle = \frac{2}{N} \begin{pmatrix} \text{Re} \langle \hat{J}_+ \rangle \\ \text{Im} \langle \hat{J}_+ \rangle \\ \langle \hat{J}_z \rangle \end{pmatrix} = \begin{pmatrix} r_x \\ r_y \\ r_z \end{pmatrix}, \quad (10)$$

where the expectation values are taken with respect to $|s_N\rangle$. Then, Eq. (8) takes the form of a closed dynamical equation of Lie-Poisson type [60–62]; that is, by defining the vector

$$\vec{h} = \begin{pmatrix} \partial_{r_x} \langle \hat{H} \rangle \\ \partial_{r_y} \langle \hat{H} \rangle \\ \partial_{r_z} \langle \hat{H} \rangle \end{pmatrix} = \nabla_{\vec{r}} \langle \hat{H} \rangle, \quad (11)$$

we can rewrite Eq. (8) as

$$\dot{\vec{r}} = -\frac{2}{\hbar N} \vec{r} \times \vec{h}. \quad (12)$$

In this representation, the restricted evolution on the AMCS manifold interestingly takes the form of a classical rigid-body equation, aka Euler's rotation equations. This formulation makes the geometric structure of the classical evolution explicit and allows for a direct comparison with classical angular-momentum and polarization dynamics.

B. Classical quantum speed limit

Now, we introduce the speed limit for the evolution governed by the restricted equations of motion in Eq. (8). We refer to the resulting quantity as the classically restricted quantum speed limit (QSL_{cl}).

In order to evaluate the trace norm in Eq. (5), we express $\partial_t |s_N\rangle = c_{\parallel} |s_N\rangle + c_{\perp} |s_N^{\perp}\rangle$ in the orthogonal basis $\{|s_N\rangle, |s_N^{\perp}\rangle\}$, accounting for the parallel and orthogonal components. This decomposition, together with

the time derivative of $|s_N\rangle$ in Eq. (7), allows us to write $\partial_t(|s_N\rangle\langle s_N|)$ as a matrix with eigenvalues $\pm|\lambda| = \pm\sqrt{N}|\dot{\alpha}_+\alpha_- - \dot{\alpha}_-\alpha_+|$. Thus, the trace norm that defines QSL_{cl} reads as

$$\text{QSL}_{\text{cl}} = \sup_{|s_N\rangle} 2|\lambda| = 2\sqrt{N} \sup_{|s_N\rangle} |\dot{\alpha}_+\alpha_- - \dot{\alpha}_-\alpha_+|. \quad (13)$$

Substituting the classical equations of motion from Eq. (8) into this expression ultimately yields the maximal rate of change of a polarization system when no quantum coherence is allowed to build up during the evolution,

$$\text{QSL}_{\text{cl}} = \frac{2}{\hbar\sqrt{N}} \sup_{|s_N\rangle} \left| \alpha_- \frac{\partial\langle\hat{H}\rangle}{\partial\alpha_+^*} - \alpha_+ \frac{\partial\langle\hat{H}\rangle}{\partial\alpha_-^*} \right|. \quad (14)$$

In the context of a classical, analytical mechanics, note that the quantity over which the supremum is taken plays the role akin to an angular momentum. Furthermore, the result enables us to compare the unrestricted QSL, Eq. (6), with its restricted counterpart QSL_{cl} from Eq. (14). In addition, we certify a nonclassicality-enabled speedup when $\text{QSL} > \text{QSL}_{\text{cl}}$ holds true, and the difference of both quantities quantifies the amount of quantum speedup.

IV. APPLICATION: CROSS-KERR EFFECT

In this section, we apply the methods developed above to the cross-Kerr effect, which, for two quantized modes, is described by the Hamiltonian

$$\hat{H}_{\text{int}} = \varepsilon \hat{n}_+ \hat{n}_-, \quad (15)$$

where $\hat{n}_\pm = \hat{a}_\pm^\dagger \hat{a}_\pm$ are the photon-number operators and ε denotes the nonlinear coupling strength [38, 63]. This interaction gives rise to nontrivial phase dynamics due to the coupling between the modes. We omit the free evolution of the modes (i.e., $\hat{H} = \hat{H}_{\text{int}}$) because a free evolution $\propto \hat{n}_+ + \hat{n}_-$ always trivially maps AMCSs to AMCSs, and we adopt natural units ($\hbar = 1$).

A. Dynamics

The full quantum evolution can be computed via the Heisenberg equation for the field operators, $\partial_t \hat{a}_\pm = -i(1 + \varepsilon \hat{n}_\mp) \hat{a}_\pm$. Therefore, up to global phases, the unrestricted evolution of an initial AMCS is given by

$$|\sigma_N(t)\rangle = \sum_{n_+=0}^N \binom{N}{n_+}^{\frac{1}{2}} \alpha_+^{n_+} \alpha_-^{n_-} e^{-i\varepsilon n_+ n_- t} |n_+, n_-\rangle, \quad (16)$$

with $\alpha_\pm = \alpha_\pm(0)$ defining the initial parameters of the AMCS. Importantly, we note that the nonlinear phase of each component $e^{-i\varepsilon n_+ n_- t} = e^{-i\varepsilon(Nn_+ - n_+^2)t}$ drives the state out of the manifold of AMCSs.

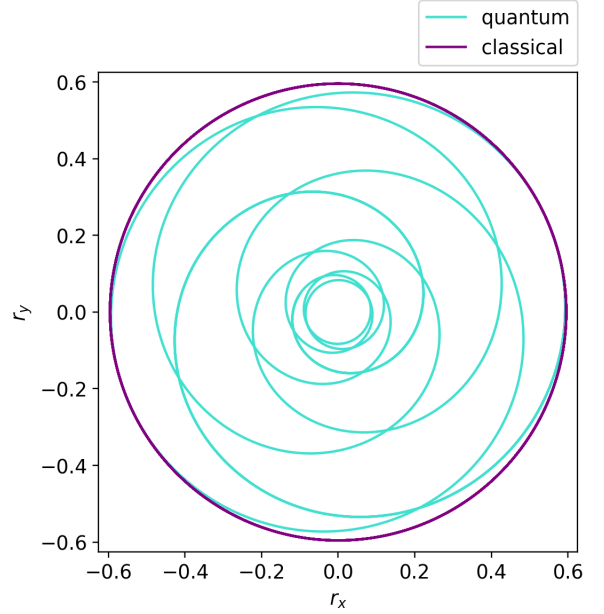


FIG. 1. Time evolution of the normalized Stokes vectors for the unrestricted (turquoise) and classical (purple) case for $\varepsilon = 0.05$ and the initial conditions $\alpha_+ = 0.95$ and $\alpha_- = 0.29 + 0.12i$. Note that the polar angle of the evolution on the Poincaré sphere is constant, and we thus only show the r_x - r_y plane.

To derive the restricted dynamics, we compute and insert $\langle\hat{H}\rangle = \varepsilon N(N-1)|\alpha_+(t)|^2|\alpha_-(t)|^2$ into Eq. (8), leading to the differential equations

$$\dot{\alpha}_\pm(t) = -iA|\alpha_\mp(t)|^2\alpha_\pm(t) \times [1 + (N-1)(|\alpha_\mp(t)|^2 - |\alpha_\pm(t)|^2)], \quad (17)$$

with $A = \varepsilon(N-1)/N$. Solving these equations reveals the constants of motion $|\alpha_\pm(t)| = |\alpha_\pm(0)| = |\alpha_\pm|$ and thus allows us to write the solution as

$$\alpha_\pm(t) = \alpha_\pm(0)e^{-i\omega_\pm t}, \quad (18)$$

with $\omega_\pm = A|\alpha_\mp|^2 [1 + (N-1)(|\alpha_\mp|^2 - |\alpha_\pm|^2)]$. Thus, the classical evolution of the AMCSs consists of a rotation in the complex plane with a constant radius,

$$|s_N(t)\rangle = \sum_{n_+=0}^N \binom{N}{n_+}^{\frac{1}{2}} \alpha_+(0)^{n_+} \alpha_-(0)^{n_-} e^{-in_+\tilde{\omega}t} |n_+, n_-\rangle, \quad (19)$$

where $\tilde{\omega} = \omega_+ - \omega_- = \varepsilon(N-1)(|\alpha_-|^2 - |\alpha_+|^2)$. We now analyze the fundamental difference between the fully quantum and the AMCS-restricted trajectories by visualization on the Poincaré sphere, describing the normalized Stokes vector \vec{r} in Eq. (10). Note that this corresponds to the Bloch sphere for spin-1/2 systems.

In Figure 1, the classically-evolved state remains on the boundary of the disc that intersects the Poincaré sphere with the r_x - r_y plane, proving that it stays classical for all

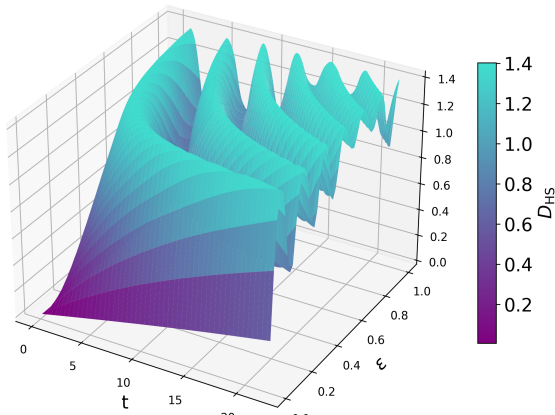


FIG. 2. Hilbert-Schmidt distance D_{HS} between classical and quantum evolutions as a function of time t and coupling strength ε for $|\alpha_+|^2 = 0.9$ and $N = 10$.

times t . In contrast, the unrestricted state erratically oscillates within the intersecting disc during the evolution, hinting at the presence of quantum coherence, which is caused by the aforementioned, highly nonlinear phases. To analyze the impact of the coupling strength ε on the difference of the classical and quantum dynamics of the states, we compute the Hilbert-Schmidt distance [64] between both evolved density operators, which reads as

$$D_{\text{HS}}(t) = \sqrt{2} \sqrt{1 - |\langle s_N(t) | \sigma_N(t) \rangle|^2} \quad (20)$$

for pure states. Figure 2 shows D_{HS} as a function of ε and t , revealing an oscillating structure that arises from the periodicity of both evolutions. The stronger the coupling, the closer $D_{\text{HS}}(t)$ oscillates near the upper limit of $\sqrt{2}$, which corresponds to perfect orthogonality between the classically evolved and quantum evolved states. For weak coupling, however, the states remain similar ($D_{\text{HS}}(t) \approx 0$) for longer times, as one would expect. Thus, we conclude that the cross-Kerr interaction introduces a nonclassical polarization evolution to the system.

B. Speed limits

To obtain the classical speed limit for a cross-Kerr interaction, we can directly substitute $\langle s_N | \hat{H} | s_N \rangle$ into Eq. (14), which gives us the following expression:

$$\text{QSL}_{\text{cl}} = 2\varepsilon \sqrt{N(N-1)} \sup_{\alpha_{\pm}} |\alpha_+ \alpha_- (|\alpha_-|^2 - |\alpha_+|^2)|. \quad (21)$$

We can straightforwardly solve this optimization problem by setting $|\alpha_+|^2 = p$ and $|\alpha_-|^2 = 1 - p$ and searching for the maximum for $p \in [0, 1]$, which is $1/4$. Thus, the maximum rate of change of a state restricted to the manifold of AMCSs in a cross-Kerr medium is explicitly

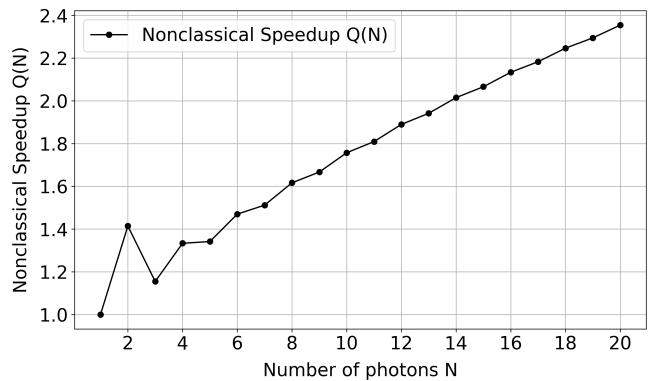


FIG. 3. Plot of the quantum speedup via the ratio $Q(N)$ of the unrestricted and the classical QSLs. Since $Q(N) > 1$, the nonclassical speedup of cross-Kerr processes is certified. The plot exhibits an advantage of even photon numbers for small photon numbers N and scales as $\mathcal{O}(N^{1/2})$ for larger N .

given by

$$\text{QSL}_{\text{cl}} = \frac{\varepsilon \sqrt{N(N-1)}}{2}. \quad (22)$$

Importantly, this limit scales linearly with ε and as $\mathcal{O}(N^{3/2})$ with the photon number N .

In contrast, the unrestricted QSL in Eq. (6) is evaluated through the eigenvalues of the Hamiltonian for a fixed N , $E(n_+) = \varepsilon n_+(N - n_+)$ with $n_+ \in [0, N]$. Thus, we find the ultimate speed limit without restrictions as

$$\text{QSL} = \varepsilon \frac{N^2 - (N \bmod 2)}{4}. \quad (23)$$

To quantitatively compare Eqs. (22) and (23), it is convenient to define the ratio

$$Q(N) = \frac{\text{QSL}}{\text{QSL}_{\text{cl}}} = \frac{N^2 - (N \bmod 2)}{2\sqrt{N(N-1)}}. \quad (24)$$

The amount to which $Q(N) > 0$ holds true certifies the speed gained through the quantum part of the evolution. Here, $Q(N)$ is strictly bigger than 1 ($\forall N > 1$), verifying a nonclassical speedup of optical cross-Kerr processes because of quantum coherence effects. Figure 3 shows the nonclassical speedup $Q(N)$, in which we can easily see the growth of $Q(N)$ as $\mathcal{O}(N^{1/2})$, cf. Eq. (24). Compared to the previous analysis for specific initial states, the QSLs used here are independent of this initial choice. Further, the ratio $Q(N)$ is even independent of the coupling strength (except for $\varepsilon = 0$, which would cause a division by zero) and thus represents a universal speedup of a cross-Kerr nonlinearity. Interestingly, we also observe the difference for odd and even N , which is more pronounced when N is small. This follows directly from the symmetric structure of the energy eigenvalues of the cross-Kerr Hamiltonian since the two degenerate maxima for odd N do not produce the highest energy eigenvalues, in contrast to the case of even N .

V. CONCLUSION

In this work, we developed a general framework to identify nonclassical speedups in polarization (likewise, angular-momentum) systems. First, we derived restricted equations of motion, which render it possible to describe the dynamics of the polarization states confined to the manifold of classical AMCSs, thus not generating or showing quantum coherence for all times t . Based on this, we were able to determine a bound to the maximal rate of change of the classical system, the classical quantum speed limit. When the quantum evolution beats this classical bound, one has a direct certification of nonclassical speedups due to polarization nonclassicality.

We applied the formalism to the cross-Kerr interaction, a prominent nonlinear dynamics in classical and quantum

polarization optics. We were able to prove a persistent nonclassical speedup, scaling as $\mathcal{O}(N^{1/2})$ with the photon number N . Thereby, we provide a quantitative measure for the quantum speedup of this process beyond classical bounds. The analysis of specific trajectories further confirms that the unrestricted evolution clearly deviates from the manifold of classical states, isolating polarization nonclassicality as the origin of the observed enhancement. The instantaneous speedups accumulate to overall faster quantum processes, saving time to reach a processing goal compared to a purely classical evolution.

ACKNOWLEDGMENTS

T.A. is grateful to the PhoQS FUTURE graduate program for financial support. J.S. and L.A. acknowledge funding through the QuantERA project QuCABOoSE.

-
- [1] M. A. Nielsen and I. L. Chuang, *Quantum Computation and Quantum Information* (Cambridge University Press, 2012) 10th Anniversary Edition.
- [2] C. Fabre and N. Treps, Modes and states in quantum optics, *Reviews of Modern Physics* **92**, 10.1103/revmodphys.92.035005 (2020).
- [3] C. Gross, Spin squeezing, entanglement and quantum metrology with bose-einstein condensates, *Journal of Physics B: Atomic, Molecular and Optical Physics* **45**, 103001 (2012).
- [4] A. Celi, A. Sanpera, V. Ahufinger, and M. Lewenstein, Quantum optics and frontiers of physics: the third quantum revolution, *Physica Scripta* **92**, 013003 (2016).
- [5] J. L. O'Brien, A. Furusawa, and J. Vučković, Photonic quantum technologies, *Nature Photonics* **3**, 687–695 (2009).
- [6] J. Wang, F. Sciarrino, A. Laing, and M. G. Thompson, Integrated photonic quantum technologies, *Nature Photonics* **14**, 273–284 (2020).
- [7] C. Noh and D. G. Angelakis, Quantum simulations and many-body physics with light, *Reports on Progress in Physics* **80**, 016401 (2016).
- [8] Y. Hasegawa, Unifying speed limit, thermodynamic uncertainty relation and heisenberg principle via bulk-boundary correspondence, *Nature Communications* **14**, 10.1038/s41467-023-38074-8 (2023).
- [9] J. Preskill, The physics of quantum information (2022).
- [10] V. Giovannetti, S. Lloyd, and L. Maccone, Quantum limits to dynamical evolution, *Physical Review A* **67**, 052109 (2003).
- [11] M. Benyoucef, Recent advances in photonic quantum technologies, *Advanced Quantum Technologies* **8**, 2400628 (2025).
- [12] A. K. Ekert, Quantum cryptography based on bell's theorem, *Physical Review Letters* **67**, 661–663 (1991).
- [13] P. W. Shor, Polynomial-time algorithms for prime factorization and discrete logarithms on a quantum computer, *SIAM Journal on Computing* **26**, 1484–1509 (1997).
- [14] L. K. Grover, A fast quantum mechanical algorithm for database search (1996), [arXiv:quant-ph/9605043](https://arxiv.org/abs/quant-ph/9605043) [quant-ph].
- [15] L. I. Mandelstam and I. E. Tamm, The uncertainty relation between energy and time in non-relativistic quantum mechanics, *Journal of Physics (USSR)* **9**, 249–254 (1945).
- [16] J. Anandan and Y. Aharonov, Geometry of quantum evolution, *Phys. Rev. Lett.* **65**, 1697–1700 (1990).
- [17] S. Deffner and S. Campbell, Quantum speed limits: from heisenberg's uncertainty principle to optimal quantum control, *Journal of Physics A: Mathematical and Theoretical* **50**, 453001 (2017).
- [18] F. Yasmin and J. Sperling, Entanglement-assisted quantum speedup: Beating local quantum speed limits, *Physical Review A* **110**, 10.1103/physreva.110.012424 (2024).
- [19] J. M. Epstein and K. B. Whaley, Quantum speed limits for quantum-information-processing tasks, *Physical Review A* **95**, 10.1103/physreva.95.042314 (2017).
- [20] D. P. Pires, E. R. deAzevedo, D. O. Soares-Pinto, F. Brito, and J. G. Filgueiras, Experimental investigation of geometric quantum speed limits in an open quantum system, *Communications Physics* **7**, 10.1038/s42005-024-01634-5 (2024).
- [21] B. Yadin, S. Imai, and O. Gühne, Quantum speed limit for states and observables of perturbed open systems, *Physical Review Letters* **132**, 230404 (2024).
- [22] D. Shrimali, B. Panda, and A. K. Pati, Stronger speed limit for observables: Tighter bound for the capacity of entanglement, the modular hamiltonian, and the charging of a quantum battery, *Physical Review A* **110**, 022425 (2024).
- [23] D. Shrimali, S. Bhowmick, and A. K. Pati, Quantum speed limit on the production of quantumness of observables, *Physical Review A* **111**, 022445 (2025).
- [24] T. Nishiyama and Y. Hasegawa, Speed limits and thermodynamic uncertainty relations for quantum systems with the non-hermitian hamiltonian, *Physical Review A* **111**, 012214 (2025).
- [25] D. Wei, H. Liu, Y. Li, F. Gao, S. Qin, and Q. Wen, Quantum speed limit for time-fractional open systems (2023).

- [26] B. Hinrichs, M. Lemm, and O. Siebert, On lieb–robinson bounds for a class of continuum fermions, *Annales Henri Poincaré* **26**, 41–80 (2024).
- [27] N. Carabba, N. Hörnedal, and A. d. Campo, Quantum speed limits on operator flows and correlation functions, *Quantum* **6**, 884 (2022).
- [28] M.-X. Luo, Quantumness speeds up quantum thermodynamics processes (2024), [arXiv:2406.13349 \[quant-ph\]](https://arxiv.org/abs/2406.13349).
- [29] C. M. Caves, Quantum-mechanical noise in an interferometer, *Physical Review D* **23**, 1693–1708 (1981).
- [30] The LIGO Scientific Collaboration, A gravitational wave observatory operating beyond the quantum shot-noise limit, *Nature Physics* **7**, 962–965 (2011).
- [31] R. Horodecki, P. Horodecki, M. Horodecki, and K. Horodecki, Quantum entanglement, *Rev. Mod. Phys.* **81**, 865–942 (2009).
- [32] L. Ares, N. Prasanna, E. Agudelo, A. Luis, B. Brecht, C. Silberhorn, and J. Sperling, Photonic entanglement and polarization nonclassicality: Two manifestations, one nature (2024), [arXiv:2407.07477 \[quant-ph\]](https://arxiv.org/abs/2407.07477).
- [33] J. Sperling and I. A. Walmsley, Classical evolution in quantum systems, *Physica Scripta* **95**, 065101 (2020).
- [34] A. Luis and A. Rivas, Angular-momentum nonclassicality by breaking classical bounds on statistics, *Phys. Rev. A* **84**, 042111 (2011).
- [35] P. W. Atkins and J. C. Dobson, Angular momentum coherent states, *Proceedings of the Royal Society of London. Series A, Mathematical and Physical Sciences* **321**, 321–340 (1971).
- [36] A. M. Perelomov, Generalized coherent states and some of their applications, *Soviet Physics Uspekhi* **20**, 703 (1977).
- [37] R. W. Boyd, *Nonlinear Optics*, 4th ed. (Academic Press, 2020).
- [38] R. Khan, F. Massel, and T. T. Heikkilä, Cross-kerr nonlinearity in optomechanical systems, *Phys. Rev. A* **91**, 043822 (2015).
- [39] S. Khorasani, Solution of cross-kerr interaction combined with parametric amplification, *Scientific Reports* **9**, 10.1038/s41598-018-38377-7 (2019).
- [40] X. L. He, Y. Lu, D. Q. Bao, H. Xue, W. B. Jiang, Z. Wang, A. F. Roudsari, P. Delsing, J. S. Tsai, and Z. R. Lin, Fast generation of schrödinger cat states using a kerr-tunable superconducting resonator, *Nature Communications* **14**, 6358 (2023).
- [41] I. Fushman and J. Vuckovic, Analysis of a quantum non-demolition measurement scheme based on kerr nonlinearity in photonic crystal waveguides, *Optics Express* **15**, 5559 (2007).
- [42] D. J. Brod, J. Combes, and J. Gea-Banacloche, Two photons co- and counterpropagating through n cross-kerr sites, *Phys. Rev. A* **94**, 023833 (2016).
- [43] M.-X. Luo, H.-R. Li, and H. Lai, Quantum computation based on photonic systems with two degrees of freedom assisted by the weak cross-kerr nonlinearity, *Scientific Reports* **6**, 29939 (2016).
- [44] K. Nemoto and W. J. Munro, Nearly deterministic linear optical controlled-not gate, *Phys. Rev. Lett.* **93**, 250502 (2004).
- [45] T. Opatrny and D.-G. Welsch, Coupled cavities for enhancing the cross-phase-modulation in electromagnetically induced transparency, *Phys. Rev. A* **64**, 023805 (2001).
- [46] M. Fleischhauer, A. Imamoglu, and J. P. Marangos, Electromagnetically induced transparency: Optics in coherent media, *Rev. Mod. Phys.* **77**, 633–673 (2005).
- [47] K. M. Beck, M. Hosseini, Y. Duan, and V. Vuletić, Large conditional single-photon cross-phase modulation, *Proceedings of the National Academy of Sciences* **113**, 9740–9744 (2016).
- [48] I.-C. Hoi, A. F. Kockum, T. Palomaki, T. M. Stace, B. Fan, L. Tornberg, S. R. Sathyamoorthy, G. Johansson, P. Delsing, and C. M. Wilson, Giant cross-kerr effect for propagating microwaves induced by an artificial atom, *Phys. Rev. Lett.* **111**, 053601 (2013).
- [49] T. Baumgratz, M. Cramer, and M. B. Plenio, Quantifying coherence, *Phys. Rev. Lett.* **113**, 140401 (2014).
- [50] J. Sperling and I. A. Walmsley, Quasiprobability representation of quantum coherence, *Physical Review A* **97**, 062327 (2018).
- [51] J. Sperling and W. Vogel, Quasiprobability distributions for quantum-optical coherence and beyond, *Physica Scripta* **95**, 034007 (2020).
- [52] J. Sperling, L. Ares, and E. Agudelo, Quasiprobabilities from incomplete and overcomplete measurements (2025).
- [53] M. Bohmann, E. Agudelo, and J. Sperling, Probing nonclassicality with matrices of phase-space distributions, *Quantum* **4**, 343 (2020).
- [54] K. C. Tan, S. Choi, and H. Jeong, Negativity of quasiprobability distributions as a measure of nonclassicality, *Physical Review Letters* **124**, 110404 (2020).
- [55] T. Linowski and L. Rudnicki, Relating the glauder-sudarshan, wigner, and husimi quasiprobability distributions operationally through the quantum-limited amplifier and attenuator channels, *Physical Review A* **109**, 023715 (2024).
- [56] J. Schwinger, *ON ANGULAR MOMENTUM*, Tech. Rep. (Harvard Univ., Cambridge, MA (United States); Nuclear Development Associates, Inc. (US), 1952).
- [57] S. Deffner and E. Lutz, Energy–time uncertainty relation for driven quantum systems, *Journal of Physics A: Mathematical and Theoretical* **46**, 335302 (2013).
- [58] S. Deffner and E. Lutz, Quantum speed limit for non-markovian dynamics, *Physical Review Letters* **111**, 010402 (2013).
- [59] A. C. da Silva, *Lectures on Symplectic Geometry*, Lecture Notes in Mathematics, Vol. 1764 (Springer Berlin, Heidelberg, 2001) pp. XII+220.
- [60] J. E. Marsden and T. S. Ratiu, *Introduction to Mechanics and Symmetry: A Basic Exposition of Classical Mechanical Systems* (Springer New York, 1999).
- [61] J. E. Marsden, S. Pekarsky, and S. Shkoller, Discrete euler-poincaré and lie-poisson equations, *Nonlinearity* **12**, 1647–1662 (1999).
- [62] D. D. Holm, J. E. Marsden, and T. S. Ratiu, The euler-poincaré equations in geophysical fluid dynamics (1999).
- [63] S. Khorasani, Solution of cross-kerr interaction combined with parametric amplification, *Scientific Reports* **9**, 1830 (2019).
- [64] J. Dajka, J. Luczka, and P. Hänggi, Distance between quantum states in the presence of initial qubit-environment correlations: A comparative study, *Phys. Rev. A* **84**, 032120 (2011).